

**This is the accepted manuscript version of the contribution published as:**

**Lohse, M., Blaser, S.R.G.A., Vetterlein, D., Schlüter, S., Oburger, E., Reemtsma, T., Lechtenfeld, O.J.** (2020):

Online nano solid phase extraction Fourier-transform ion cyclotron resonance mass spectrometry workflow to analyze small scale gradients of soil solution organic matter in the rhizosphere

*Anal. Chem.* **92** (15), 10442 – 10449

**The publisher's version is available at:**

<http://dx.doi.org/10.1021/acs.analchem.0c00946>

# On-line nano-solid phase extraction Fourier-transform ion cyclotron resonance mass spectrometry workflow to analyze small scale gradients of soil solution organic matter in the rhizosphere

M. Lohse<sup>1</sup>; S. R. G. A. Blaser<sup>2</sup>; D. Vetterlein<sup>2,3</sup>; S. Schlüter<sup>2</sup>; E. Oburger<sup>4</sup>; T. Reemtsma<sup>1,5</sup>; O. J. Lechtenfeld<sup>\*1,6</sup>

<sup>1</sup> Department of Analytical Chemistry, Helmholtz Centre for Environmental Research – UFZ, 04318, Leipzig, Germany

<sup>2</sup> Department of Soil System Science, Helmholtz Centre for Environmental Research – UFZ, 06120, Halle, Germany

<sup>3</sup> Institute of Agricultural and Nutritional Sciences, Martin-Luther-University Halle-Wittenberg, Von-Seckendorff-Platz 3, 06120 Halle (Saale), Germany

<sup>4</sup> Institute of Soil Research, University of Natural Resources and Life Sciences, Vienna – BOKU, 3430 Tulln an der Donau, Austria

<sup>5</sup> Institute of Analytical Chemistry, University of Leipzig, 04103, Leipzig, Germany

<sup>6</sup> ProVIS – Centre for Chemical Microscopy, Helmholtz Centre for Environmental Research – UFZ, 04318, Leipzig, Germany

\*Corresponding Author: oliver.lechtenfeld@ufz.de

## Abstract

A new method combining on-line nano-solid phase extraction coupled with Fourier-transform ion cyclotron resonance mass spectrometry (FT-ICR-MS) was developed to extract and analyze organic matter (OM) from microliter volumes of salt containing soil solution samples. The system allows the reproducible analysis of only minute amounts of organic carbon (down to 10 ng C) without the need of further sample preparation. The new method was applied to unravel developing small-scale patterns of dissolved organic matter (DOM) in soil solution of a soil column experiment in which *Zea mays* plants were grown for three weeks. Soil solution was sampled by micro suction cups from the undisturbed soil-root system once a week. Growth of the root system and, hence, position of individual roots relative to the suction cups was followed by X-ray computed tomography (X-ray CT). Our method allowed resolving the chemical complexity of soil solution OM (up to 4300 molecular formulas). This makes it possible to observe chemical gradients in the rhizosphere on a molecular level over time. The increasing influence of roots on soil solution OM is visible from higher molecular masses, an increasing degree of oxygenation and a higher fraction of formulas containing heteroatoms. The on-line nano-solid phase extraction-FT-ICR-MS method

40 provides novel insight into the processes affecting DOM in the rhizosphere, such as  
41 root exudation, microbial processes, and soil organic matter stabilization.

42

43 Soil organic matter (SOM) formation and composition are highly influenced by the  
44 interaction with plants via the root system. Comparison of biomarkers for roots and  
45 shoots indicates that root-derived carbon dominates organic matter (OM) formation in  
46 agricultural soils compared to above-ground litter.<sup>1</sup> The presence of bioavailable  
47 carbon sources, such as root exudates, for soil microorganisms can influence the  
48 microbial growth strategy, suggesting a strong effect of root exudation on microbial  
49 communities.<sup>2</sup>

50 The temporal and spatial heterogeneity in the rhizosphere (i.e. the soil influenced by  
51 roots) has already been studied in terms of chemical composition,<sup>3</sup> nutrient level,<sup>4</sup>  
52 physical parameters like hydraulic properties,<sup>5</sup> oxygen,<sup>6</sup> and pH,<sup>7</sup> as well as in the  
53 organization of microbial communities.<sup>8</sup> It is apparent that analyzing root mediated  
54 processes requires a time resolved, non-destructive sampling operating on the small  
55 spatial scale of the rhizosphere (0.5 – 4 mm).<sup>9</sup>

56 Soil solution is a highly dynamic component of the rhizosphere, enabling mass flux of  
57 carbon and nutrients. Direct sampling of soil solution (e.g. via micro suction cups  
58 (MSC)) yields *in situ* information about the rhizosphere state and processes<sup>10,11</sup> like  
59 nutrient dynamics<sup>12,4</sup> and organic acids turnover.<sup>13,10</sup> As an alternative to MSC, micro-  
60 dialysis has also been applied to sample the dynamic pools of enzymes,<sup>14</sup> nutrients<sup>15</sup>,  
61 and amino acids.<sup>16</sup> A non-targeted view into the vast number of organic components  
62 present in the rhizosphere would help to reveal the complex interplay of root mediated  
63 carbon input, microbial degradation, and carbon sequestration beyond the individual  
64 compound level.

65 Previous non-target studies of soil solution OM used sample collection by suction cups,  
66 subsequent solid phase extraction (SPE) and analysis by FT-ICR-MS.<sup>17</sup> SPE by  
67 packed sorbents is a standard method to desalt and enrich aqueous OM samples.<sup>18</sup>  
68 Hyphenation of SPE and MS measurements has been demonstrated for OM utilizing  
69 a liquid chromatography (LC)-system.<sup>19</sup> An automated on-line micro-extraction by  
70 packed sorbents was used for the direct analysis of salt rich marine samples at the  
71 scale of 2 mL sample volume.<sup>20</sup> However, a further downscaling of packed column  
72 SPE workflows for enrichment and desalting of OM-samples does not seem feasible

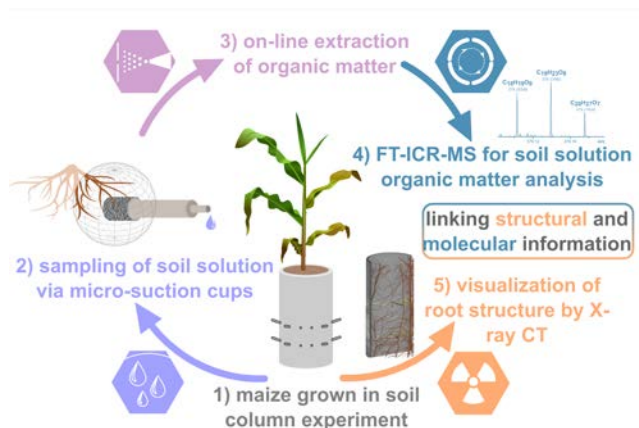
73 due to the high risk of sample contamination and a lack of commercially available solid  
74 phases with less than one mg of sorbent mass.

75 Bailey et al. presented results for the direct infusion (DI) analysis of soil solution utilizing  
76 FT-ICR-MS.<sup>21</sup> However, high and varying salt concentrations usually limits the  
77 application of direct infusion of samples into the mass spectrometer due to ionization  
78 suppression.<sup>22,23</sup> It is also possible to study the organic carbon distributions in soil  
79 samples using destructive extraction based or imaging methods.<sup>24–26</sup> A workflow for an  
80 on-line extraction method for small quantities of solid soil samples was recently  
81 presented by Shen et al. who utilized on-line supercritical fluid extraction mass  
82 spectrometry (SFE-LC-FT-MS) for the analysis down to 1 mg of soil.<sup>27</sup>

83 All approaches to analyze soil solution or soil OM mentioned above either require  
84 several milliliters of sample volume or use destructive methods for sample acquisition  
85 and thus lack the required spatial and temporal resolution needed to reveal the  
86 processes caused by the interplay of root structure and OM in the rhizosphere.

87 The aim of this study was to develop a sample preparation and measurement workflow  
88 for the extraction of OM from a few microliters of soil solution. Analysis via FT-ICR-MS  
89 allows for a non-targeted molecular insight into small scale rhizosphere processes  
90 despite the high salt concentrations in the soil solution samples. To account for the  
91 limited (microliter) sample volume and its high ratio of salt to organic carbon (approx.  
92 100:1 m/m) a robust and sensitive on-line nano-SPE-FT-ICR-MS based workflow for  
93 the on-line extraction and direct analysis of soil solution OM was developed and  
94 validated.

95 The combination of molecular information from FT-ICR-MS with the structural data of  
96 the root system as provided by X-ray computed tomography (X-ray CT) will allow for  
97 the first time a non-destructive, time resolved analysis of complex rhizosphere  
98 biogeochemical processes at high spatial resolution (Figure 1).



99

100 **Figure 1:** Workflow to link information about root structure to changes in the molecular  
 101 composition of soil solution OM in the rhizosphere. It consists of: 1) growing maize in soil  
 102 columns, 2) sampling of soil solutions via micro-suction cups and 3) apply on-line extraction of  
 103 OM (on-line nano-SPE) with 4) subsequent analysis of soil solution OM by ultra-high resolution  
 104 FT-ICR-MS and 5) X-ray CT to visualize the root structure.

## 105 **Experimental section**

### 106 **Samples**

107 Soil solution samples were collected three times (7 d, 14 d, 21 d) at 16 cm below the  
 108 soil surface during a three week growth of *Zea mays* in a soil column experiment.  
 109 Experimental details on the preparation of the soil column experiment, the soil solution  
 110 sampling, X-ray CT<sup>12,28</sup>, and anion chromatography can be found in the supporting  
 111 information (SI) to this article.

112 Suwannee River Fulvic Acid-standard (SRFA II, International Humic Substances  
 113 Society, 20 mg L<sup>-1</sup>, approx. 10 mg L<sup>-1</sup> carbon) was used for the on-line nano-SPE  
 114 method development. For the evaluation of eluent composition, formic acid  
 115 concentration, and comparison to DI-ESI measurements a SRFA concentration of 10  
 116 mg L<sup>-1</sup> was used. Although not a soil solution OM, SRFA represents a well  
 117 characterized complex OM mixture.<sup>29</sup>

118 Effective separation of salts from OM was tested by adding sodium chloride (NaCl, 1  
 119 g L<sup>-1</sup>) to SRFA, similar to OM-to-salt ratios (1:100, min. 25 mg L<sup>-1</sup> dissolved organic  
 120 carbon (DOC)) determined in soil solutions. Total salt concentration was approximated  
 121 based on the anion concentration assuming that all anions are present as the  
 122 respective sodium salt (max: 2.5 g L<sup>-1</sup> salts). SRFA and soil solution samples were  
 123 diluted with the aqueous eluent (1:2, water with 0.005 vol-% formic acid) immediately  
 124 prior to analysis.

## 125 **Chemicals**

126 Details regarding all the used chemicals can be found in the SI (Table S1).

## 127 **On-line nano-solid phase extraction**

128 The nano-LC system (Ultimate 3000 nanoRSLC, Thermo Fischer Scientific, Waltham,  
129 MA, U.S.A.) consisted of a pump and autosampler with 5  $\mu\text{L}$  sample loop. The sample  
130 was retained on a C-18 precolumn (Acclaim™ PepMap™ 100, 2 cm x 75  $\mu\text{m}$ , 3  $\mu\text{m}$ ,  
131 Thermo Fischer Scientific, Waltham, MA, U.S.A.) and eluted with 90% MeOH, 10%  
132 water (both with 0.005 vol-% formic acid). A 10-way valve was used to direct the salt  
133 containing matrix to the waste while allowing the OM-fraction to pass to the nano-ESI  
134 source and FT-ICR-MS.

135 The nano-LC gradient was modified to allow separation of salts from OM in a low  
136 overall run time (29 min) while ensuring stable and reproducible spray conditions. For  
137 the washing and equilibration steps, the flow rate was set to 1500  $\text{nL min}^{-1}$ . During the  
138 elution of OM the flow rate was lowered to 200  $\text{nL min}^{-1}$  in order to allow sufficient time  
139 for the acquisition of scans in the FT-ICR-MS. After the OM was eluted the flow rate  
140 was increased again to flush the system. HPLC-grade water and methanol with 0.005  
141 vol-% formic acid (pH of aqueous eluent 3.4 at 22 °C) were used as eluents. Eluents  
142 with pH 8 (2 mM ammonium acetate adjusted with  $\text{NH}_4\text{OH}$ ), pH 4 (2 mM ammonium  
143 formate adjusted with formic acid), and pH 6.22 (no additives to eluent) were compared  
144 to test the effect of the eluent pH on the extraction reproducibility. A scheme of the  
145 nano-LC setup is shown in Figure S1 and the gradient conditions are provided in Table  
146 S2.

## 147 **FT-ICR-MS-measurements**

148 All MS measurements were performed with an FT-ICR mass spectrometer with a  
149 dynamically harmonized analyzer cell (solariX XR, Bruker Daltonics, Billerica, MA,  
150 U.S.A.) and a 12 T refrigerated actively shielded superconducting magnet (Bruker  
151 Biospin, Wissembourg, France). The mass spectrometer was controlled with  
152 ftmsControl 2.2.0 (Bruker Daltonics, MA, U.S.A.). Mass spectra were recorded in the  
153 mass range setting 147 – 1000  $m/z$  in magnitude mode (four megaword time domain,  
154 1.677 s transient length) and reduced profile mode (97% data reduction). External  
155 mass calibration was done with SRFA. A nano-electrospray ionization (nano-ESI)  
156 source for the nano-LC-coupling, CaptiveSpray-Source (Bruker Daltonics, Billerica,  
157 MA, U.S.A.), was used in negative mode. Parameters for the Captive Spray nano-ESI

158 source were as follows: dry gas temperature: 150 °C, dry gas flow rate: 3.0 L min<sup>-1</sup>,  
159 capillary voltage: 1300 V. The same conditions were applied for the nano-solid phase  
160 extraction and DI-nano-ESI measurements. For DI-nano-ESI measurements the C-18  
161 precolumn was removed from the nano-LC system.

## 162 **DI-ESI-FT-ICR-MS measurements**

163 A standard ESI source (Apollo II, Bruker Daltonics, Billerica, MA, U.S.A.) in negative  
164 ionization mode (capillary voltage: 4.3 kV, flow rate: 240 μL h<sup>-1</sup>, dry gas temperature:  
165 200 °C, dry gas flow rate: 3.0 L min<sup>-1</sup>, nebulizer gas flow rate: 1.0 bar) was used for  
166 direct infusion measurements. For one mass spectrum 256 scans were co-added in  
167 the mass range 147–1000 m/z.

## 168 **Data processing**

169 Mass spectra from LC acquisition runs were averaged from 7 to 15 min (approx. 247  
170 single scans) to generate the mass spectrum of the OM-containing fraction.

171 Internal re-calibration of averaged spectra was done with a list of masses commonly  
172 present in natural organic matter (m/z 250–600,  $n = 188$ , linear calibration function).

173 The root mean square error (RMSE) of the calibration masses was below 0.2 ppm.

174 Peaks were considered detected if the signal-to-noise ( $S/N$ ) ratio was greater than four.

175 Raw spectra were processed with Compass DataAnalysis 5.0 (Bruker Daltonics, MA,  
176 U.S.A.).

177 Molecular formulas (MF) were assigned to peaks in the range 150–750 m/z allowing  
178 for elemental compositions C<sub>1–60</sub> H<sub>0–122</sub> O<sub>0–40</sub> N<sub>0–2</sub> S<sub>0–1</sub> with an error range of ±0.5 ppm  
179 according to Lechtenfeld et al.<sup>30</sup> and Koch et al.<sup>31</sup> Briefly, the following rules were  
180 applied:  $0.3 \leq H/C \leq 3.0$ ,  $0 \leq O/C \leq 1.2$ ,  $0 \leq N/C \leq 1.5$ ,  $0 \leq DBE \leq 25$  (double bond  
181 equivalent,  $DBE = 1 + 1/2 (2C - H + N)$ , Koch et al.),<sup>32</sup>  $-10 \leq DBE-O \leq 10$  (Herzprung  
182 et al.<sup>33</sup>), and element probability rules proposed by Kind and Fiehn.<sup>34</sup> Isotope formulas  
183 were removed from the data set as they represent duplicate chemical information. The  
184 mass error range in the final data set was limited to the 5<sup>th</sup>–95<sup>th</sup> percentile of errors of  
185 CHO formulas in the initial data set (here approx. ± 0.45 ppm).  $S/N$  for the soil solution  
186 analysis was set to 8 as explained in the results and discussion section. All MF present  
187 in the MSC or eluent blank samples were removed from the final data set.

188

## 189 **Results and Discussion**

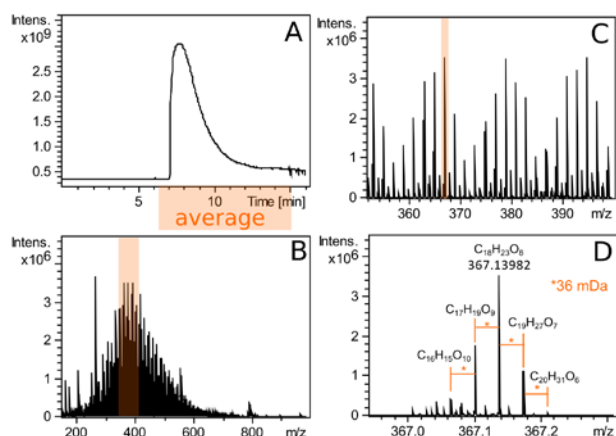
### 190 **Optimization of the on-line nano-solid phase extraction method**

191 Most studies focusing on the characterization of OM apply direct infusion-(DI)-ESI FT-  
192 ICR-MS after removal of salt and OM enrichment via SPE.<sup>35</sup> Enrichment and desalting  
193 are crucial as ionization of OM can be largely suppressed by salts.<sup>23</sup> However,  
194 extraction of OM from soil solution samples from column experiments of only 50 – 150  
195  $\mu\text{L}$  could not be achieved with a conventional off-line micro-SPE and subsequent DI-  
196 nano-ESI measurement (using 10 mg sorbent, Figure S2). Although OM-signals were  
197 detected, contaminant peaks and salt clusters dominated the mass spectrum resulting  
198 in low sensitivity and incomplete coverage of OM complexity. Combining the benefits  
199 of an automated miniaturized SPE for desalting with the low risk of contamination was  
200 possible using a nano-LC-nano-ESI system which can be directly hyphenated with a  
201 mass spectrometer. The main advantage of a nano-LC-system is the low flow rate  
202 which allows injection and analysis of small sample volumes with limited dilution of the  
203 analytes prior to injection. In addition, nano-ESI offers a higher tolerance for buffers  
204 and salt as well as increased sensitivity compared to ESI.<sup>36</sup> For FT-ICR-MS  
205 hyphenation, the low flow rate allows for more scans and a higher intensity per sample  
206 volume since the duty cycle of the MS is mostly limited by the ion detection speed and  
207 not their accumulation time.

208 Figure 2A shows an example chromatogram and the averaged mass spectrum of 20  
209  $\text{mg L}^{-1}$  SRFA with 1  $\text{g L}^{-1}$  of NaCl of the optimized method using eluents with pH 3.4.  
210 As discussed, the most important factor is the ability of the method to remove salts  
211 from the soil solutions. It was possible to generate a mass spectrum with a typical OM  
212 pattern (Figure 2B-D). A 100-fold excess of salt over organic carbon was present while  
213 injecting only 5  $\mu\text{L}$  of sample. The total amount of organic carbon needed to generate  
214 the mass spectrum was just 25 ng. This is more than three orders of magnitude less  
215 material than required by the recently published on-line SFE-LC-FT-MS-workflow.<sup>27</sup>

216





217  
 218 **Figure 2:** Extraction and measurement of OM samples with the on-line nano-SPE method at  
 219 pH 3.4. (A) Total ion count (TIC). (B) Averaged full scan FT-ICR mass spectrum (7 – 15 min,  
 220 250 scans). (C) Zoom into the mass spectrum (m/z 340 – 400) with regular patterns of OM.  
 221 (D) Zoom into nominal mass 367 (most intensive OM peak). Mass spacing of 36 mDa  
 222 (indicated by an asterisk) represents the mass difference of an exchange of “O” vs “CH<sub>4</sub>” as  
 223 indicated by the ion formulas of the CHO class. 20 mg L<sup>-1</sup> SRFA with 1 g L<sup>-1</sup> NaCl, 5 μL injection  
 224 volume, diluted 1:2 with aqueous eluent (water with 0.005 vol-% formic acid).

225 Even from 10 ng of organic carbon with a 600-fold excess of salt (6 g L<sup>-1</sup>) a spectrum  
 226 with the typical OM pattern could be obtained (Figure S3) showing the feasibility of our  
 227 on-line nano-SPE method for even smaller amounts of carbon and matrices with higher  
 228 salt content. Further increasing salt concentration in the sample led to a loss in the  
 229 number of assigned MF (Figure S4) so that sample dilution was required (see below).

### 230 *Optimization of the solvent composition*

231 DI-ESI experiments using SRFA (10 mg L<sup>-1</sup>) were performed to determine the optimal  
 232 solvent composition for OM analysis. The highest number and highest reproducibility  
 233 of MF were obtained using 90% MeOH (Table S3). This agrees with previous findings  
 234 that a high organic solvent fraction is advantageous for ESI analysis of OM.<sup>37</sup> Adding  
 235 a buffer to the eluent (e.g. ammonium formate, pH 4) decreased the number of  
 236 assigned MF significantly for negative ionization mode due to signal suppression.<sup>38</sup>  
 237 However, diluted formic acid (0.005 vol-%, pH ~ 3.4) is already sufficient to keep the  
 238 pH of OM solutions constant despite the acidic functional groups of the components in  
 239 SRFA (Figure S5), while minimizing ion suppression (Figure S6).

### 240 *Optimization of the eluent pH*

241 The effect of pH of the eluent was tested for a range of pH values (4, 6, and 8, Figure  
 242 S7). Although a similar number of MF (5300) could be assigned after on-line extraction

243 of OM (20 mg L<sup>-1</sup> SRFA with 1 g L<sup>-1</sup> NaCl) for all three pH values tested, the fraction of  
244 shared formulas between triplicate measurements at each pH varied between 1728  
245 (33% of all unique formulas), 1018 (19%) and 1380 (26%) for pH 8, 6 and 4  
246 respectively. A low pH generally favors the retention of humic and fulvic acids.<sup>39</sup>  
247 However, the number of nitrogen-containing formulas was slightly higher at pH 8 (7.9%  
248 of MF) as compared to pH 4 (5.4%) indicating an increase of retention- and/or  
249 ionization efficiency for basic compounds at higher pH (Figure S7).

250 To allow for a complete protonation of acidic components and an overall better  
251 retention and reproducibility on a C-18 phase a formic acid buffer at pH 3.4 was used  
252 for further analysis. The applied one-step-“elution” of OM with 90% methanol has two  
253 major advantages i) it allows for fast run times as most OM fractions elute together and  
254 ii) it provides constant eluent composition for ESI and hence less discrimination due to  
255 varying ionization conditions.<sup>40,37</sup> The elution of OM in one step for an on-line extraction  
256 is thus different from an actual chromatography of OM as described in literature for off-  
257 line,<sup>41</sup> offline 2D-<sup>42</sup> and on-line LC separations.<sup>43,44</sup>

#### 258 **FT-ICR-MS parameter optimization for on-line extraction**

259 Mass resolution and mass accuracy in FT-ICR-MS are strongly depended on the  
260 number of ions in the ICR cell, which can be controlled via the ion accumulation time  
261 (IAT).<sup>45</sup>

##### 262 *Optimization of the ion accumulation time*

263 The high sensitivity of the FT-ICR-MS allows that soil solutions can even be diluted  
264 before the on-line extraction to lower the salt concentration. The corresponding  
265 decrease in organic carbon concentration may be compensated for by increasing the  
266 IAT. To find the optimal ratio between dilution and IAT, a mixture of 20 mg L<sup>-1</sup> SRFA  
267 with 1 g L<sup>-1</sup> NaCl was diluted with the aqueous eluent and processed with the on-line  
268 nano-SPE and FT-ICR-MS measurements at different IATs. As expected, increasing  
269 the IAT led to a larger number of assigned MF (Table 1). The results indicate that the  
270 reduction of ion suppression via sample dilution has a larger effect than the loss of  
271 sensitivity on the number of detected MF. Since all the samples were diluted with the  
272 aqueous eluent, an undiluted sample has a higher pH (~ 5.2, Figure S5), the OM is  
273 less retained and as a result, a lower number of formulas could be assigned.

274

275 **Table 1:** Effect of dilution of a 20 mg L<sup>-1</sup> SRFA sample with 1 g L<sup>-1</sup> NaCl and variation in ion  
 276 accumulation time (IAT) on the molecular formula (MF) assignment and the intensity weighted  
 277 averaged (WA) molecular parameters. The aqueous eluent (water with 0.005 vol-% formic  
 278 acid) was used for dilution.

Dilution factor	none	2	2	5	10
IAT (ms)	10	5	10	25	35
number of MF	1902	2182	3003	3731	3976
RMSE of assigned formulas (ppb)	200	190	174	179	172
Intensity of highest OM Peak <i>m/z</i> 363.1449 (10 <sup>5</sup> )	7.3	3.4	7.9	16	18
TIC (10 <sup>8</sup> )	7.1	5.4	7.3	11.6	12.8
WA <i>m/z</i>	440.8	462.7	467.6	457.7	451
WA O/C	0.36	0.41	0.42	0.44	0.45
WA H/C	1.24	1.18	1.14	1.12	1.13

279 RMSE: root mean squared error, TIC: total ion count

280  
 281 Expectedly, higher IAT resulted in increased peak intensities (e.g. as indicated from  
 282 the total ion count (TIC)) while the RMSE of formula assignments remained at sub-  
 283 ppm level (Table 1). However, the mass error distribution at high IAT (above 25 ms)  
 284 reveals a bimodal pattern, likely due to a too high number of ions of the ICR cell (8).  
 285 All the spectra were dominated by formulas of the CHO class. With increasing IAT a  
 286 higher number of heteroatom containing MF could be observed (Figure S9).

#### 287 *Optimization of the sample dilution*

288 To account for possible variation in the organic carbon concentration of soil solutions,  
 289 three replicates of SRFA and a soil solution were analyzed at 2- and 4-fold dilution  
 290 using the on-line nano-SPE method. While the number of assigned MF in the soil  
 291 solutions seems to be independent of the dilution (dilution 1:2 and 1:4 tested), the  
 292 reproducibility of the number of shared formulas between three measurement  
 293 replicates was at a maximum after a 1:2 dilution of the samples (Table S4). Decreasing  
 294 carbon concentration due to dilution did not affect the quality of OM mass spectra. The  
 295 two soil solution samples and the SRFA sample grouped acceptably according to their  
 296 aggregated molecular parameters (Table S4). We conclude that our method is robust  
 297 against DOC concentration variability among different soil solution samples.

298 The major difference between the replicate measurement of a soil solution and SRFA  
299 was the higher fraction of MF unique for a single measurement (Table S4). Increasing  
300 the *S/N* threshold of MF in the final data set reduced the number of unique assignments  
301 (Figure S10). As a compromise between the number of assigned MF and non-  
302 reproducible peaks, the *S/N* threshold for the analysis of soil solutions was set to eight  
303 resulting in 50% MF shared between triplicate measurements. For SRFA the increase  
304 of the *S/N* threshold led to 61 % shared formulas between triplicates, while for the  
305 higher dilution level of the soil solution the reproducibly remained lower at 38% (Table  
306 S4).

307 This value is lower than reported for DI-ESI FT-ICR-MS measurement.<sup>37</sup> In contrast to  
308 published values of mass spectral reproducibility, we cannot distinguish extraction and  
309 MS effects on reproducibility, and a small influence of the sample matrix cannot be  
310 excluded for our on-line method. Another explanation for the lower spectral  
311 reproducibility is the data reduction during MS acquisition as differences in baseline  
312 noise between replicates affects the number of detected signals irrespective of a post-  
313 measurement *S/N* filtering.

314 For further analysis of soil solution samples with the on-line workflow all samples were  
315 diluted 2-fold, the IAT set to 10 ms, and *S/N* threshold set to 8.

### 316 **Comparison between on-line nano-solid phase extraction and direct infusion** 317 **measurements**

318 To assess systematic differences between our on-line nano-SPE and the conventional  
319 DI-ESI method six replicates of SRFA were analyzed with both methods.

320 A similar number of MF could be assigned in SRFA for the on-line nano-SPE as  
321 compared to a DI measurement (Table 2). Mass accuracy and mass-resolving power  
322 was slightly lower during the on-line extraction which can be explained by the  
323 averaging of a transient signals with variable ion numbers causing small shifts of the  
324 ion cyclotron frequencies.<sup>46</sup>

325 The on-line nano-SPE method generally resulted in a higher intensity weighted  
326 average (WA) H/C ratio and a lower O/C ratio compared to the DI-ESI (Table 2). This  
327 effect can mostly attributed to the different ion sources (nano-ESI vs conventional ESI),  
328 source parameters, and solvent composition used.<sup>37,47</sup> An additional, however smaller,  
329 bias of the nano-LC pre-column on the OM composition was also observed (Figure  
330 S11). In addition, the average *m/z* of assigned MF also increased by 20% with the new

331 on-line nano-SPE workflow as compared to DI-ESI measurements, indicating a better  
 332 coverage of the OM mass distribution. Since standard DI-ESI is also inevitably  
 333 selective on the determined OM composition, the difference caused by the application  
 334 of different ionization sources was expected.<sup>47</sup>

335 **Table 2:** Comparison of the new on-line nano-solid phase extraction workflow and DI-ESI  
 336 regarding spectral quality, number of molecular formulas (MF), Intensity weighted average  
 337 (WA) molecular composition (mean  $\pm$  standard derivation,  $n = 6$ ). For the on-line nano-SPE 20  
 338 mg L<sup>-1</sup> SRFA was prepared in water (10 ms IAT). For the DI-ESI measurements 10 mg L<sup>-1</sup>  
 339 SRFA was prepared in 50% MeOH / 50% water (15 ms IAT).

Sample introduction to FT-ICR-MS	On-line nano-SPE	Direct infusion ESI
Number of MF	3045 $\pm$ 153	2951 $\pm$ 177
RMSE formula assignment (ppb)	148.7 $\pm$ 13.2	108.4 $\pm$ 1.93
Mass-Resolving power at $m/z$ 400 $\pm$ 1	432783 $\pm$ 27102	480881 $\pm$ 38919
WA $m/z$	503.7 $\pm$ 2.2	391.38 $\pm$ 10.2
WA H/C	1.196 $\pm$ 0.009	1.112 $\pm$ 0.006
WA O/C	0.388 $\pm$ 0.007	0.469 $\pm$ 0.014
Volume of Sample consumed per run ( $\mu$ L)	2.5	31
Mass of carbon used for spectrum generation (ng) per run	25	155

340  
 341 For one SRFA-standard without salt addition, we tested if a fractionation of OM on the  
 342 C-18 phase may contribute to the observed differences in molecular composition  
 343 (Table 2, Figure S11) between the two methods. The applied gradient program for the  
 344 on-line extraction resulted in a hydrophilic fraction eluting at high water content (99%)  
 345 whereas the later eluting hydrophobic fraction (90% MeOH) contributed to the majority  
 346 of the total intensity (Figure S12). The majority of MF (98%) was detected in the  
 347 hydrophobic fraction indicating no major loss of molecular information from highly polar  
 348 OM compounds due to the on-line extraction method.

349 The early elution of very polar compounds was also observed applying an on-line LC-  
 350 ESI-FT-ICR-MS method for the separation of OM.<sup>44</sup> As the hydrophilic fraction is co-  
 351 eluting with salts, highly polar OM may not be detected with our method. Raeke et al.  
 352 showed that when applying standard off-line SPE protocols, small and very polar

353 compound classes like carbohydrates have very low SPE recoveries and are also  
354 negatively biased in DI-ESI-FT-ICR-MS.<sup>23</sup>

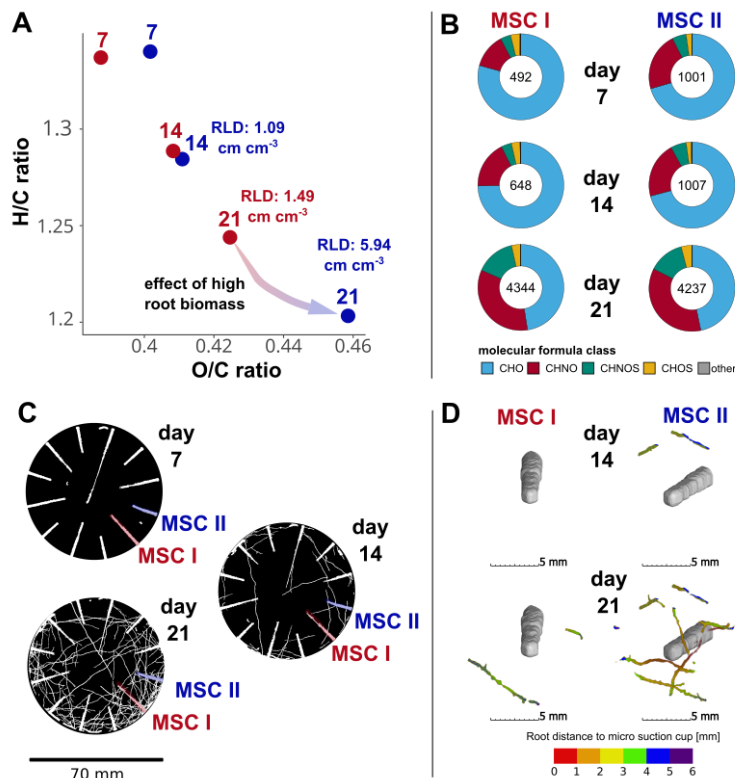
355 Alternatively to OM extraction, also direct sample infusion in negative ion mode after  
356 dilution with methanol (i.e. without extraction) could be an option for OM analysis if the  
357 sample is not acidified with mineral acids (e.g. HCl).<sup>21</sup> Using our soil solution samples  
358 with approx. 2.5 g L<sup>-1</sup> of salt DI-ESI-FT-ICR mass spectra were dominated by salt  
359 clusters. In contrast, our on-line nano-SPE method achieves a much cleaner spectrum  
360 and a larger number of OM-signals (Figure S13), demonstrating the necessity of an  
361 extraction step for soil solution samples.

### 362 **Application of the method to soil solution samples from column experiments**

363 The on-line nano-SPE-FT-ICR-MS method was applied to study chemical gradients of  
364 OM developing in the rhizosphere during plant growth in a soil column experiment.  
365 Two micro suction cup positions (MSC I and II) were selected based on the X-ray CT  
366 images (Figure 3A, B). According to X-ray CT maize roots developed in the proximity  
367 of both MSCs between day 7 and day 21 of the growth experiment, with a higher root  
368 density around MSC II (Figure 3C, D, Figure S14). For each sampling time, 2.5 µL soil  
369 solution collected from the MSCs were measured with on-line nano-SPE-FT-ICR-MS.  
370 Between 500 and 4300 MF were assigned within the mass range of 150 to 750 Da  
371 (Figure 3B). Although the on-line extraction only used 2.5 µL of soil solution sample,  
372 approximately twice as many formulas could be assigned as compared to published  
373 results using off-line extraction of rhizosphere soil.<sup>24</sup>

374 With increasing root biomass the composition of the OM shifted towards higher O/C  
375 and lower H/C ratios in both MSCs (Figure 3A). This trend was stronger for MSC II with  
376 a higher root length density (RLD; 5.94 cm cm<sup>-3</sup>) than MSC I (1.49 cm cm<sup>-3</sup>) at day 21  
377 (Figure 3A). The detected differences in the aggregated elemental ratios regarding the  
378 time series and the different RLD were always larger than the replicate measurement  
379 variability (Table 2, Table S4).

380



381

382 **Figure 3:** Soil solution OM gradient during plant growth: application of on-line nano-SPE A)  
 383 Peak intensity weighted aggregated van Krevelen diagrams for soil solution samples of three  
 384 time points (7 d, 14 d, 21 d, number above circles) and two MSCs (I: red, II: blue) of the same  
 385 *Zea mays* plant. B) Relative ratio of molecular formula (MF) classes (CHO: blue, CHNO: red,  
 386 CHNOS: cyan, CHOS: yellow, other: gray) for all six samples. The number in the center of the  
 387 charts are the total number of MF. C) 3D X-ray CT-images with 2D maximum intensity  
 388 projections in the soil layer defined by the MSCs at 16 cm below the soil surface. Roots and  
 389 MSCs have the same X-ray attenuation and both structures appear white in the images. A  
 390 larger version of the projections is available in the SI (Figure S14). D) 3D reconstruction of the  
 391 roots close to the two MSC. Roots inside a cube ( $V = 1 \text{ cm}^3$ ) around the MSC tips are shown,  
 392 and colors indicate the distance of the respective root segment to the center of the MSC.

393

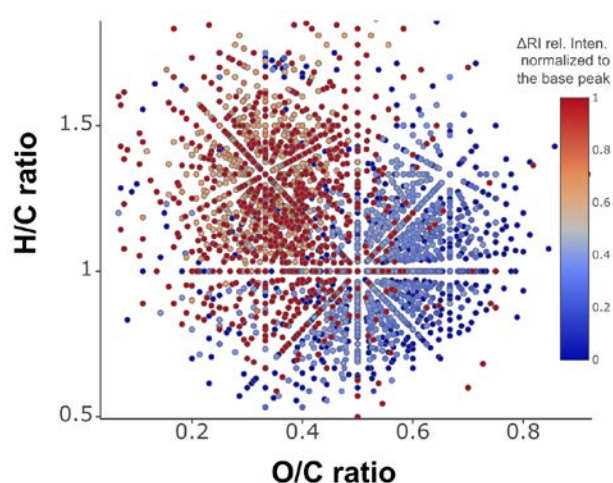
394 The 5-fold difference of the local RLD in the soil volume accessible by the MSC I and  
 395 II was mirrored in a distinct occurrence of MF assigned to MSC I and II samples (Figure  
 396 4). Expectedly also the intensity ratio of MF present in both MSC samples (I and II)  
 397 showed the same trend towards higher O/C and lower H/C ratios (Figure 4) which  
 398 could also be observed for the other soil solution samples (Figure S15).

399 Next to root-derived carbon, all soil solution samples also contained a background of  
 400 complex soil solution OM with extensive isobaric overlap. However, the addition of  
 401 oxygen-rich root-derived molecules was easily detected already at the nominal mass

402 level (Figure S16). Similarly, an addition of new, oxygen rich molecules (which were  
403 not present at day 7) to the soil solution was observed (Figure 3B, Figure 4, Table S5,  
404 Figure S17).

405 In addition, to the higher degree of oxygenation in rhizosphere OM, Kaplan et al.<sup>24</sup> also  
406 showed that rhizosphere OM had a higher WA molecular weight compared to soil less  
407 influenced by roots. We could observe a similar trend regarding the WA molecular  
408 weight over the growth period of three weeks. The high fraction of heteroatom  
409 containing MF in the rhizosphere also matched our findings (Figure 3B and Table S5).

410



411

412 **Figure 4:** Overlay of van Krevelen diagrams for the two analyzed soil solutions from MSC I  
413 and II on day 21. Molecular formulas (MF) unique for a high root biomass in the proximity of  
414 the MSC (MSC II, dark blue, 701) and a lower root biomass (MSC I, dark red, 808) are  
415 highlighted. MF were the base peak normalized relative intensity is more than 50 % higher  
416 intensity in one sample is colored either: blue (MSC II, 979) or red (MSC I, 490). MF with no  
417 significant difference in the intensity (2067) are not shown.

418

419 The potential of the new method was demonstrated by showing trends in the soil  
420 solution OM composition related to RLD and root age. Despite the numerous analytical  
421 challenges like the background of soil OM, a high salt-to-OM ratio, and a low sample  
422 volume, our workflow revealed temporal and spatial trends in the molecular  
423 composition. The comparison of soil solutions from two nearby MSCs with contrasting  
424 root length density demonstrated the advantage of sampling a small soil solution  
425 volume to obtain new spatially resolved insights into rhizosphere processes.



## 426 **Conclusions**

427 We presented an on-line nano-solid phase extraction FT-ICR-MS workflow that can  
428 analyze OM from small sample volumes (down to 1  $\mu\text{L}$ ) without any additional sample  
429 preparation. The low pH of the eluent used in the method allows for a reproducible on-  
430 line extraction and MS measurement. To lower the overall salt content, samples can  
431 be diluted with the aqueous eluent without sacrificing sensitivity or spectral quality.  
432 Utilizing the potential to increase the IAT for FT-ICR-MS measurement makes it  
433 possible to detect thousands of MF in a single sample. The amount of carbon needed  
434 for an on-line extraction and measurement of OM was lowered by a factor of six as  
435 compared to DI-ESI measurements. More importantly, the low amount of consumed  
436 sample enables us to obtain high spatial precision and coverage of the root system.

437 Combining visualization of the root structure via X-ray CT with the analysis of soil  
438 solution OM by FT-ICR-MS, as demonstrated here, resulted in molecular insights into  
439 early rhizosphere development. The low sample consumption of our method allows  
440 resolving patterns of OM at spatial scales of the root system, which was not possible  
441 before due to much larger sample consumption for soil solution OM analysis or  
442 destructive sampling.

443 Our workflow enables the study of chemical gradients in space and time directly in a  
444 soil context. The low sample consumption of our method made it possible to also  
445 analyze the soil solution samples for nutrients (Table S5). We will now be able to link  
446 the release and transformation of OM with the nutrient status of the rhizosphere to gain  
447 a more complete picture of interlinked processes in the root-soil system. Additional  
448 mass spectrometric information may be generated by applying a nano-LC separation  
449 as well as additional measurements in positive ionization mode. Combining this  
450 analysis with the detailed structural insight provided by X-ray CT can deepen our  
451 understanding of the complex dynamics of SOM formation in the rhizosphere.

452 The combination of the on-line nano-SPE method with non-target or targeted analysis  
453 of other complex samples by FT-ICR-MS is a powerful tool, especially for fields like  
454 metabolomics. The method can be used where sample volume is limited and salt  
455 concentrations are high such as single-cell analysis<sup>48</sup> or sediment pore water.<sup>49</sup>

## 456 **Supporting Information**

457 Experimental details on the preparation of the soil column experiment, the soil solution  
458 sampling, and the X-ray CT measurement as well as additional tables and figures.

- 460 (1) Mendez-Millan, M.; Dignac, M.-F.; Rumpel, C.; Rasse, D. P.; Derenne, S.  
461 Molecular dynamics of shoot vs. root biomarkers in an agricultural soil estimated  
462 by natural abundance <sup>13</sup>C labelling. *Soil Biol. Biochem.* **2010**, *42*, 169–177.
- 463 (2) Blagodatskaya, E. V.; Blagodatsky, S. A.; Anderson, T.-H.; KUZYAKOV, Y.  
464 Contrasting effects of glucose, living roots and maize straw on microbial growth  
465 kinetics and substrate availability in soil. *Eur. J. Soil Sci.* **2009**, *60*, 186–197.
- 466 (3) Angst, G.; Kögel-Knabner, I.; Kirfel, K.; Hertel, D.; Mueller, C. W. Spatial  
467 distribution and chemical composition of soil organic matter fractions in  
468 rhizosphere and non-rhizosphere soil under European beech (*Fagus sylvatica*  
469 L.). *Geoderma* **2016**, *264*, 179–187.
- 470 (4) Llanderal, A.; García-Caparrós, P.; Contreras, J. I.; Segura, M. L.; Teresa Lao, M.  
471 Spatio-temporal variations in nutrient concentration in soil solution under  
472 greenhouse tomato. *J. Plant Nutr.* **2019**, *42*, 842–852.
- 473 (5) Moradi, A. B.; Carminati, A.; Lamparter, A.; Woche, S. K.; Bachmann, J.;  
474 Vetterlein, D.; Vogel, H.-J.; Oswald, S. E. Is the Rhizosphere Temporarily Water  
475 Repellent? *Vadose Zone J.* **2012**, *11*, 0.
- 476 (6) Uteau, D.; Hafner, S.; Pagenkemper, S. K.; Peth, S.; Wiesenberg, G. L. B.;  
477 Kuzyakov, Y.; Horn, R. Oxygen and redox potential gradients in the rhizosphere  
478 of alfalfa grown on a loamy soil. *Z. Pflanzenernähr. Bodenk.* **2015**, *178*, 278–  
479 287.
- 480 (7) Hinsinger, P.; Plassard, C.; Tang, C.; Jaillard, B. Origins of root-mediated pH  
481 changes in the rhizosphere and their responses to environmental constraints: A  
482 review. *Plant Soil* **2003**, *248*, 43–59.
- 483 (8) Kuzyakov, Y.; Blagodatskaya, E. Microbial hotspots and hot moments in soil:  
484 Concept & review. *Soil Biol. Biochem.* **2015**, *83*, 184–199.
- 485 (9) Kuzyakov, Y.; Razavi, B. S. Rhizosphere size and shape: Temporal dynamics  
486 and spatial stationarity. *Soil Biol. Biochem.* **2019**, *135*, 343–360.
- 487 (10) Schulz, H.; Vetterlein, D. Analysis of organic acid concentration with time in  
488 small soil-solution samples from the rhizosphere of maize (*Zea mays* L.). *Z.*  
489 *Pflanzenernähr. Bodenk.* **2007**, *170*, 640–644.
- 490 (11) Vetterlein, D.; Jahn, R. Gradients in soil solution composition between bulk soil  
491 and rhizosphere – In situ measurement with changing soil water content. *Plant*  
492 *Soil* **2004**, *258*, 307–327.
- 493 (12) Gao, W.; Blaser, Sebastian R. G. A.; Schlüter, S.; Shen, J.; Vetterlein, D. Effect  
494 of localised phosphorus application on root growth and soil nutrient dynamics in  
495 situ – comparison of maize (*Zea mays*) and faba bean (*Vicia faba*) at the  
496 seedling stage. *Plant Soil* **2019**.
- 497 (13) Dessureault-Rompré, J.; Nowack, B.; Schulin, R.; Luster, J. Modified micro  
498 suction cup/rhizobox approach for the in-situ detection of organic acids in  
499 rhizosphere soil solution. *Plant Soil* **2006**, *286*, 99–107.
- 500 (14) Buckley, S.; Allen, D.; Brackin, R.; Jämtgård, S.; Näsholm, T.; Schmidt, S.  
501 Microdialysis as an in situ technique for sampling soil enzymes. *Soil Biol.*  
502 *Biochem.* **2019**, *135*, 20–27.
- 503 (15) Inselsbacher, E.; Öhlund, J.; Jämtgård, S.; Huss-Danell, K.; Näsholm, T. The  
504 potential of microdialysis to monitor organic and inorganic nitrogen compounds in  
505 soil. *Soil Biol. Biochem.* **2011**, *43*, 1321–1332.
- 506 (16) Warren, C. R. Development of online microdialysis-mass spectrometry for  
507 continuous minimally invasive measurement of soil solution dynamics. *Soil Biol.*  
508 *Biochem.* **2018**, *123*, 266–275.

- 509 (17) Thieme, L.; Graeber, D.; Hofmann, D.; Bischoff, S.; Schwarz, M. T.; Steffen, B.;  
510 Meyer, U.-N.; Kaupenjohann, M.; Wilcke, W.; Michalzik, B.; Siemens, J.  
511 Dissolved organic matter characteristics of deciduous and coniferous forests with  
512 variable management: different at the source, aligned in the soil. *Biogeosciences*  
513 **2019**, *16*, 1411–1432.
- 514 (18) Dittmar, T.; Koch, B.; Hertkorn, N.; Kattner, G. A simple and efficient method for  
515 the solid-phase extraction of dissolved organic matter (SPE-DOM) from  
516 seawater. *Limnol. Oceanogr. Methods* **2008**, *6*, 230–235.
- 517 (19) Swenson, M. M.; Oyler, A. R.; Minor, E. C. Rapid solid phase extraction of  
518 dissolved organic matter. *Limnol. Oceanogr. Methods* **2014**, *12*, 713–728.
- 519 (20) Morales-Cid, G.; Gebefugi, I.; Kanawati, B.; Harir, M.; Hertkorn, N.; Rosselló-  
520 Mora, R.; Schmitt-Kopplin, P. Automated microextraction sample preparation  
521 coupled on-line to FT-ICR-MS: application to desalting and concentration of river  
522 and marine dissolved organic matter. *Anal. Bioanal. Chem.* **2009**, *395*, 797–807.
- 523 (21) Bailey, V. L.; Smith, A. P.; Tfaily, M.; Fansler, S. J.; Bond-Lamberty, B.  
524 Differences in soluble organic carbon chemistry in pore waters sampled from  
525 different pore size domains. *Soil Biol. Biochem.* **2017**, *107*, 133–143.
- 526 (22) Sleighter, R. L.; McKee, G. A.; Hatcher, P. G. Direct Fourier transform mass  
527 spectral analysis of natural waters with low dissolved organic matter. *Org.*  
528 *Geochem.* **2009**, *40*, 119–125.
- 529 (23) Raeke, J.; Lechtenfeld, O. J.; Wagner, M.; Herzsprung, P.; Reemtsma, T.  
530 Selectivity of solid phase extraction of freshwater dissolved organic matter and  
531 its effect on ultrahigh resolution mass spectra. *Environ. Sci.: Processes Impacts*  
532 **2016**, *18*, 918–927.
- 533 (24) Kaplan, D. I.; Xu, C.; Huang, S.; Lin, Y.; Tolić, N.; Roscioli-Johnson, K. M.;  
534 Santschi, P. H.; Jaffé, P. R. Unique Organic Matter and Microbial Properties in  
535 the Rhizosphere of a Wetland Soil. *Environ. Sci. Technol.* **2016**, *50*, 4169–4177.
- 536 (25) Mueller, C. W.; Kölbl, A.; Hoeschen, C.; Hillion, F.; Heister, K.; Herrmann, A. M.;  
537 Kögel-Knabner, I. Submicron scale imaging of soil organic matter dynamics  
538 using NanoSIMS – From single particles to intact aggregates. *Org. Geochem.*  
539 **2012**, *42*, 1476–1488.
- 540 (26) Veličković, D.; Anderton, C. R. Mass spectrometry imaging: Towards mapping  
541 the elemental and molecular composition of the rhizosphere. *Rhizosphere* **2017**,  
542 *3*, 254–258.
- 543 (27) Shen, Y.; Zhao, R.; Tolić, N.; Tfaily, M. M.; Robinson, E. W.; Boiteau, R.; Paša-  
544 Tolić, L.; Hess, N. J. Online supercritical fluid extraction mass spectrometry  
545 (SFE-LC-FTMS) for sensitive characterization of soil organic matter. *Faraday*  
546 *Discuss.* **2019**, *218*, 157–171.
- 547 (28) Gao, W.; Schlüter, S.; Blaser, Sebastian R. G. A.; Shen, J.; Vetterlein, D. A  
548 shape-based method for automatic and rapid segmentation of roots in soil from  
549 X-ray computed tomography images: Routine. *Plant Soil* **2019**.
- 550 (29) Averett, R. C.; Leenherr, J. A.; McKnight, D. M.; Thorn, K. A. *Humic substances*  
551 *in the Suwannee River, Georgia; interactions, properties, and proposed*  
552 *structures*, 1994.
- 553 (30) Lechtenfeld, O. J.; Kattner, G.; Flerus, R.; McCallister, S. L.; Schmitt-Kopplin, P.;  
554 Koch, B. P. Molecular transformation and degradation of refractory dissolved  
555 organic matter in the Atlantic and Southern Ocean. *Geochim. Cosmochim. Acta*  
556 **2014**, *126*, 321–337.
- 557 (31) Koch, B. P.; Dittmar, T.; Witt, M.; Kattner, G. Fundamentals of molecular formula  
558 assignment to ultrahigh resolution mass data of natural organic matter. *Anal.*  
559 *Chem.* **2007**, *79*, 1758–1763.

- 560 (32) Koch, B. P.; Kattner, G.; Witt, M.; Passow, U. Molecular insights into the  
561 microbial formation of marine dissolved organic matter: recalcitrant or labile?  
562 *Biogeosciences* **2014**, *11*, 4173–4190.
- 563 (33) Herzsprung, P.; Hertkorn, N.; Tümpling, W. von; Harir, M.; Friese, K.; Schmitt-  
564 Kopplin, P. Understanding molecular formula assignment of Fourier transform  
565 ion cyclotron resonance mass spectrometry data of natural organic matter from a  
566 chemical point of view. *Anal. Bioanal. Chem.* **2014**, *406*, 7977–7987.
- 567 (34) Kind, T.; Fiehn, O. Seven Golden Rules for heuristic filtering of molecular  
568 formulas obtained by accurate mass spectrometry. *BMC Bioinform.* **2007**, *8*, 105.
- 569 (35) Li, Y.; Harir, M.; Lucio, M.; Kanawati, B.; Smirnov, K.; Flerus, R.; Koch, B. P.;  
570 Schmitt-Kopplin, P.; Hertkorn, N. Proposed Guidelines for Solid Phase Extraction  
571 of Suwannee River Dissolved Organic Matter. *Anal. Chem.* **2016**, *88*, 6680–  
572 6688.
- 573 (36) Wilm, M.; Mann, M. Analytical Properties of the Nano-electrospray Ion Source.  
574 *Anal. Chem.* **1996**, *68*, 1–8.
- 575 (37) Kido Soule, M. C.; Longnecker, K.; Giovannoni, S. J.; Kujawinski, E. B. Impact of  
576 instrument and experiment parameters on reproducibility of ultrahigh resolution  
577 ESI FT-ICR mass spectra of natural organic matter. *Org. Geochem.* **2010**, *41*,  
578 725–733.
- 579 (38) Mallet, C. R.; Lu, Z.; Mazzeo, J. R. A study of ion suppression effects in  
580 electrospray ionization from mobile phase additives and solid-phase extracts.  
581 *Rapid Commun. Mass Spectrom.* **2004**, *18*, 49–58.
- 582 (39) Hawkes, J. A.; Patriarca, C.; Sjöberg, P. J. R.; Tranvik, L. J.; Bergquist, J.  
583 Extreme isomeric complexity of dissolved organic matter found across aquatic  
584 environments. *Limnol. Oceanogr. Lett.* **2018**, *3*, 21–30.
- 585 (40) Brown, T. L.; Rice, J. A. Effect of Experimental Parameters on the ESI FT-ICR  
586 Mass Spectrum of Fulvic Acid. *Anal. Chem.* **2000**, *72*, 384–390.
- 587 (41) Koch, B. P.; Ludwiczowski, K.-U.; Kattner, G.; Dittmar, T.; Witt, M. Advanced  
588 characterization of marine dissolved organic matter by combining reversed-  
589 phase liquid chromatography and FT-ICR-MS. *Mar. Chem.* **2008**, *111*, 233–241.
- 590 (42) Spranger, T.; van Pinxteren, D.; Reemtsma, T.; Lechtenfeld, O. J.; Herrmann, H.  
591 2D Liquid Chromatographic Fractionation with Ultra-high Resolution MS Analysis  
592 Resolves a Vast Molecular Diversity of Tropospheric Particle Organics. *Environ.*  
593 *Sci. Technol.* **2019**, *53*, 11353–11363.
- 594 (43) Patriarca, C.; Bergquist, J.; Sjöberg, P. J. R.; Tranvik, L.; Hawkes, J. A. Online  
595 HPLC-ESI-HRMS Method for the Analysis and Comparison of Different  
596 Dissolved Organic Matter Samples. *Environ. Sci. Technol.* **2018**, *52*, 2091–2099.
- 597 (44) Kim, D.; Kim, S.; Son, S.; Jung, M.-J.; Kim, S. Application of Online Liquid  
598 Chromatography 7 T FT-ICR Mass Spectrometer Equipped with Quadrupolar  
599 Detection for Analysis of Natural Organic Matter. *Anal. Chem.* **2019**, *91*, 7690–  
600 7697.
- 601 (45) Vladimirov, G.; Hendrickson, C. L.; Blakney, G. T.; Marshall, A. G.; Heeren, R.  
602 M. A.; Nikolaev, E. N. Fourier transform ion cyclotron resonance mass resolution  
603 and dynamic range limits calculated by computer modeling of ion cloud motion.  
604 *J. Am. Soc. Mass Spectrom.* **2012**, *23*, 375–384.
- 605 (46) Masselon, C.; Tolmachev, A. V.; Anderson, G. A.; Harkewicz, R.; Smith, R. D.  
606 Mass measurement errors caused by “local” frequency perturbations in FTICR  
607 mass spectrometry. *J. Am. Soc. Mass Spectrom.* **2002**, *13*, 99–106.
- 608 (47) Hertkorn, N.; Frommberger, M.; Witt, M.; Koch, B. P.; Schmitt-Kopplin, P.;  
609 Perdue, E. M. Natural organic matter and the event horizon of mass  
610 spectrometry. *Anal. Chem.* **2008**, *80*, 8908–8919.

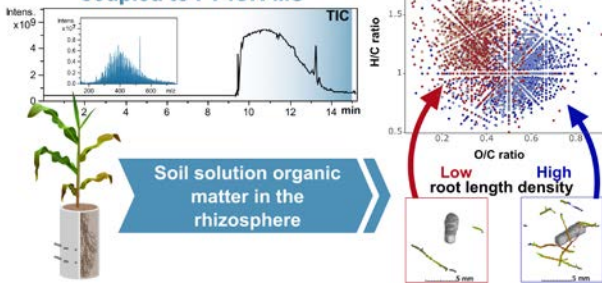
- 611 (48) Dusny, C.; Lohse, M.; Reemtsma, T.; Schmid, A.; Lechtenfeld, O. J. Quantifying  
612 a Biocatalytic Product from a Few Living Microbial Cells Using Microfluidic  
613 Cultivation Coupled to FT-ICR-MS. *Anal. Chem.* **2019**, *91*, 7012–7018.
- 614 (49) Rossel, P. E.; Bienhold, C.; Boetius, A.; Dittmar, T. Dissolved organic matter in  
615 pore water of Arctic Ocean sediments: Environmental influence on molecular  
616 composition. *Org. Geochem.* **2016**, *97*, 41–52.

## 617 **Acknowledgements**

618 The authors are grateful for using the analytical facilities of the Centre for Chemical  
619 Microscopy (ProVIS) at the Helmholtz Centre for Environmental Research, Leipzig  
620 which is supported by the European Regional Development Funds (EFRE - Europe  
621 funds Saxony) and the Helmholtz Association. Furthermore, the authors are grateful  
622 for Frank Hochholdinger for the supply of *Zea mays* seeds. We gratefully acknowledge:  
623 Jan Kaesler, Limei Han and Maria Paula da Silva for their help with the FT-ICR-MS  
624 method development, Eva Lippold for the support during the soil column experiment,  
625 Michaela Wunderlich for performing the anion chromatography analysis, Kai Franze  
626 for the data processing support, the UFZ Workshop for construction of the columns as  
627 well as Elaine Jennings for proofreading the manuscript. We would like to thank the  
628 reviewers for their thoughtful comments.

629 This project was carried out in the framework of the priority programme 2089  
630 “Rhizosphere spatiotemporal organisation - a key to rhizosphere functions” funded by  
631 DFG (project numbers: 403669053, 403801423, and 403803214).

**On-line nano-solid phase extraction coupled to FT-ICR-MS**



632

633 For Table of Contents only

634

635